Chapter 4
Thermal Propulsion

The thrust from thermal propulsion engines, such as jet engines, results from the exhaust of propellant gases, which is achieved by the rapid expansion of the heated gas. The heat usually comes from the combustion of chemical propellants—which we will assume in the following without loss of generality—or from the supply of external heat, or from both. A chemical propellant, therefore, serves two different purposes at the same time: it is a provider of mass for the required mass flow rate and a provider of energy to accelerate itself to ejection velocity.

We now want to know how an engine converts combustion heat into thrust, that is, how the expansion of propellant gases can be described in terms of thermodynamics, and how, with a given amount of energy in the combustion chamber, we can determine and maximize the thrust of the propulsion with an adequate combustion chamber and nozzle design. In doing so, we will first assume a propulsion engine with an arbitrarily formed combustion chamber and nozzle. It is not important for us how the propellant actually gets into the chamber, but we merely assume that it somehow appears there with a given mass rate $\dot{m}_p$, and that it carries a certain amount of energy per mole, which, upon combustion. heats it. The energy might even be supplied externally. The total received thermal energy per mole of propellant mass is the molar enthalpy, which we label h_0. The conditions mentioned above generally apply to mono-, and bipropellant, hybrid, dual mode, and thermoelectric thrusters. Even cold gas propulsion is applicable if one considers the product of pressure times molar volume in the combustion chamber as a molar enthalpy. Actually, we have the following (see Fig. 4.1):

Essential engine requirements A propellant gas with a known pressure p_0, a received molar enthalpy h_0, and excited internal degrees of freedom n (see Eq. (4.1.2)) flows with mass flow rate $\dot{m}_p$ and with sound velocity (see Eq. (4.1.13)) through a narrow throat having cross section A_t, and escapes through a widening nozzle by means of controlled expansion. This constrictional geometry is called a *Laval nozzle*.

U. Walter, *Astronautics*, https://doi.org/10.1007/978-3-319-74373-8_4

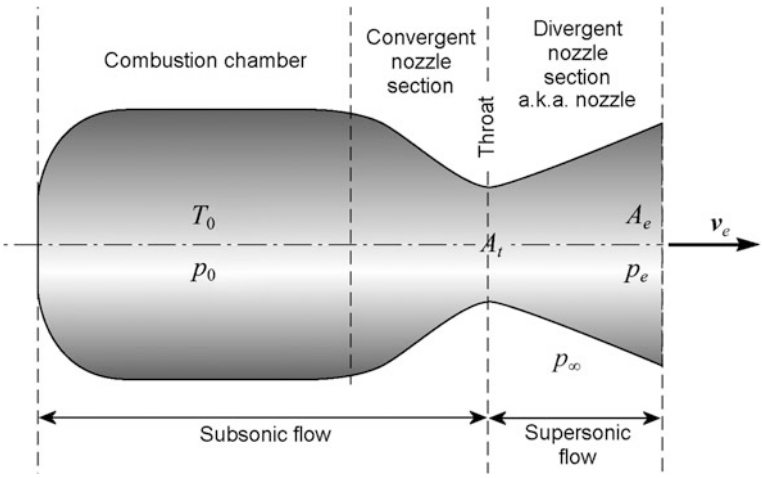

Fig. 4.1 Thrust chamber with Laval nozzle: sections and parameters

This chapter deals with understanding the behavior of the propellant gas in such an engine, and its optimal design for maximum thrust. Section 4.1 will follow the gas flow from the combustion chamber (index 0), through the throat of the combustion chamber (index t, throat) along the nozzle to the nozzle exit (index e, exit), and outside (index ∞) (see Fig. 4.1). In Sects. 4.2 and 4.4, we will analyze the optimal engine design after having determined the thrust of a thermal engine in Sect. 4.3.

4.1 Engine Thermodynamics

4.1.1 Physics of Propellant Gases

The properties of a thermal thruster are essentially determined by the properties of the propellant gas while flowing through the engine, from the combustion chamber right down to the nozzle exit. In order to understand the thrust characteristics, we therefore need to understand the basic behavior of a gas. Let us have a look at the physical and chemical characteristics of a propellant gas, before we apply this knowledge to calculate the thrust and optimize the design of the engine. The theory we will lay out below is based on the assumption that we have an *ideal engine*.

An **ideal thermal engine** is characterized by:

- The propellant is an ideal gas. In particular no viscous effects occur.
- Any change of gas state is adiabatic (heat losses to the walls are negligible).
- No frictional losses, no boundary layer losses.
- The gas is spatially homogeneous in the chamber.
- The gas flow is one-dimensional, i.e. the flow is axisymmetric.
- Gas properties (in particular the drift velocity) are constant across any plane normal to the flow.
- Steady gas flow at the exit of the combustion chamber and beyond (i.e. no shock waves).
- The gas composition does not change in space and time after combustion.
- No multi-phase flow (i.e., no liquid drops or solid particles in the gas).
- The acceleration of the rocket is negligible compared to acceleration of the gas.

In addition we assume (if not stated otherwise) that there is no beam divergence at the nozzle exit. In terms of Sect. 1.3.3 this all means that

$$\overline{v}_e = v_e$$
$$\eta_{div} = \eta_{VDF} = \zeta_d = \zeta_v = 1$$

Due to the last assumption our theory is a one-dimensional theory of gas flow, which allows us to describe spatial conditions in the engine by only one variable, i.e., the distance traveled along the engine axis.

Ideal Gas Thermodynamics

With these assumptions we are now going to exploit the behavior of the gas along the engine axis. Because the gas is ideal, the so-called *intensive thermodynamic variables* pressure p, gas density $\rho = m_p/V$, and gas temperature T (variables not depending on the amount of gas, in contrast to those which do depend on the amount of gas such as gas mass and volume, the so-called *extensive thermodynamic variables*) are interdependent as described by the ideal gas law:

$$p = \rho \frac{R}{M_p} T \quad \textbf{ideal gas law} \tag{4.1.1}$$

with

R **universal gas constant** with value $R = 8.314\ \mathrm{J\,K^{-1}mol^{-1}}$

M_p **molar mass** (mass per mole = mass per 6.022×10^{23} molecules) of the propellant

When the gas pressure forms due to combustion in the chamber, and when the gas thermally expands along the nozzle axis, internal energy, pressure, density, and temperature are constantly changing. We assume that the corresponding conversion

processes are reversible and adiabatic. Physically speaking, such processes are called isentropic—they preserve entropy. The thermodynamic potential that adequately describes an isentropic process is the so-called enthalpy. It encompasses the internal energy U (thermal energy) of the gas, which corresponds to the microscopic, statistical motion of the molecules and internal molecular energy, plus the macroscopic displacement work pV of the gas, but not its macroscopic flow energy (kinetic energy). The enthalpy H and the molar enthalpy h of an ideal gas with mass m_p are given by

$$H := U + pV = m_p c_p T \tag{4.1.2}$$

and

$$h = \frac{\kappa}{\kappa - 1} RT$$

with

$$c_p = \frac{\kappa}{\kappa - 1} \frac{R}{M_p} \quad \textit{specific thermal heat capacity} \text{ at constant pressure}$$

$$\kappa = \frac{c_p}{c_V} = 1 + \frac{2}{n} \approx 1 + \frac{2}{8} = 1.25 \quad \textbf{heat capacity ratio}$$

c_V *specific thermal heat capacity* at constant volume
n average number of **excited degrees of freedom** of the gas molecules

Molecular Degrees of Freedom

The number of excited degrees of freedom n of the gas particles is an important characteristic of the gas, since it determines in how many micromechanical forms thermal energy is stored in the gas. So, n, as well as the heat capacity ratio, may be considered as a indicator of the energy storage capacity of the gas molecules. As will be seen in a moment, among other things, this determines the temperature of the gas. The value of n depends on the specific type and composition of the gas. A propellant gas is usually composed of different types of molecules. Each gas component can move in all three directions in space, so it always has three translatory degrees of freedom $n_{trans} = 3$. If the gas component is monatomic, the atom is not able to take up any more internal energies (gas ionization can be neglected in propellant engines), and $n = n_{trans} = 3$. For diatomic molecules there are two additional rotational degrees of freedom $n_{rot} = 2$(two rotational axes perpendicular to the molecular axis—the rotation around the molecular axis does not count, as quantum-mechanically there exists no corresponding moment of inertia), and one vibrational degree of freedom along the molecular axis, $n_{vib} = 1$, so in total $n = 6$. Polyatomic molecules mostly have a three-dimensional configuration, and thus three rotational axes and three vibrational degrees of freedom, so $n = 9$. Two important exceptions, however, are: the linear CO_2 molecule with $n_{rot} = 2$ and $n_{vib} = 1$, therefore $n = 6$, and the important planar H_2O

with $n_{rot} = 3$ and $n_{vib} = 2$, implying $n = 8$. For a propellant gas mixture the actual number of degrees of freedom is a stoichiometric average over all gas components, so in general it is not integer.

If you heat up a gas, the heat energy is distributed via collisions evenly between the molecules to cause translational, rotational, and vibrational motion. According to the equipartition theorem of statistical mechanics each degree of freedom of a particle, be it translatory, rotational, or vibrational, has the same average energy in thermal equilibrium, namely $\frac{1}{2}k_BT$, no matter how massive the particle. But only translational motion determines the temperature of the gas. Physically speaking, the temperature of a gas is the kinetic energy of the average microscopic, translational motion, the so-called root-mean-square velocity v_{rms}, i.e., of the velocity of its molecules, only. The corresponding relation is

$$\frac{n_{trans}}{2}k_BT = \frac{1}{2}m_p v_{rms}^2$$

where k_B is the Boltzmann constant. If one were able to limit the motion of the gas to a line or a surface, it would therefore have the translational energy $\frac{1}{2}k_BT$ and $\frac{2}{2}k_BT$, respectively. Generally, gas can move freely in all three dimensions, in case of which it possesses $\frac{3}{2}k_BT$ translational energy. Although rotational and vibrational motions physically also constitute energy, they do not contribute to temperature. Nevertheless, they altogether make up the internal energy U of the gas. Because there is no lower limit to translational energy and since the quantum energy of molecule rotation is very low, translational and rotational modes are always excited. Quantum vibrational energies are much higher and start to get excited at around 800 K. Therefore at intermediate temperatures the number of excited degrees of freedom increases while κ monotonously decreases with increasing temperatures. Dissociation of molecules starts at about 2500 K and finally at extremely high temperatures, beyond 9000 K, which do not occur in thrusters, one also would have to consider ionizing degrees of freedom, i.e., gas plasma.

The number of theoretically accessible degrees of freedom of the molecules is between 3 for monatomic noble gases and 9 for three-dimensional polyatomic molecules, or equivalently $1.22 \leq \kappa \leq 1.67$. We therefore arrive at the following rule of thumb:

> Due to the high combustion chamber temperatures, almost all degrees of freedom of the mostly polyatomic molecules are excited, and as the gas is also a mixture of different components, $n \approx 8$ is a good average value for any rocket propellant with the corresponding heat capacity ratio $\kappa \approx 1.25$.

Two examples are: $n(O_2/H_2) = 7.41$, $n(O_2/N_2H_4) = 8.70$, where X/Y denotes all reaction components of the oxidant X and the propellant Y. In the first case, the

planarity of the resulting water molecule is obviously responsible for a relatively low number of degrees of freedom.

Example

What is the heat capacity ratio of dry air at standard conditions?

The molar composition of dry air is 78% N_2, 21% O_2 and 1% Ar, which is 99% diatomic molecules with excited degrees of freedom $n = 5$ (at ambient temperature the one vibration mode is not excited at room temperature) and 1% atoms with $n = 3$. So we find $\kappa_{air} = 0.99 \cdot 1.400 + 0.01 \cdot 1.667 = 1.403$. This is exactly the value as given in relevant tables of thermodynamics.

Thermal Efficiency

On the path from the combustion chamber along the nozzle to the exit, the energy of the gas is continuously converted: Internal energy (heat) is converted into gas expansion work pV and macroscopic flow energy, and the other way round. Thereby the intensive thermodynamic variables T, p, and ρ change in line with the gas Eq. (4.1.1) and the macroscopic drift velocity v changes as well. In physics the so-called *thermal efficiency* η (a.k.a. *thermodynamic* or *ideal cycle efficiency*) describes how efficiently internal energy (heat) is converted into work and gas flow in course of these energy changes. As we assume only adiabatic (isentropic) processes the following thermodynamic relations hold:

$$\eta = 1 - \frac{T}{T_0} = 1 - \left(\frac{p}{p_0}\right)^{\frac{2}{n+2}} = 1 - \left(\frac{\rho}{\rho_0}\right)^{\frac{2}{n}} \leq 1 \quad \textbf{thermal efficiency} \tag{4.1.3}$$

From this follows

$$\rho = \rho_0 (1 - \eta)^{n/2} \tag{4.1.4}$$

In the following, it would be rather tedious to express the thermodynamic equations either by p (which is appropriate in most circumstances), or by T, or by ρ. We want to free ourselves from this ambivalence by the following convention

> We use the thermal efficiency η as a substitute for p, T and ρ, which permits us to always and immediately shift to any of these intensive thermodynamic variables by the application of Eq. (4.1.3).

In this way η is like a convenient exchange currency. This representation also has the very practical benefit of considerably simplifying the equations, though the equations derived will look quite different from those in the literature. Therefore for the most important equations, we will also cite them in their familiar notation.

4.1.2 Flow Velocity

Let v be the gas flow velocity (drift velocity) and T its temperature at any point along the engine axis. According to the general law of the conservation of energy the total energy, i.e., the kinetic energy (macroscopic flow energy) plus the enthalpy of the gas, expressed by the state variables v, T, has to be the same as in the combustion chamber (v_0, T_0)

$$\frac{1}{2}m_p v_0^2 + m_p c_p T_0 = \frac{1}{2}m_p v^2 + m_p c_p T \tag{4.1.5}$$

Assuming that the gas flow velocities in the combustion chamber at the location of heat generation are negligibly small, $v_0 \approx 0$, we derive from this the gas flow velocity at any position in the engine

$$v^2 = 2c_p T_0 \left(1 - \frac{T}{T_0}\right) = 2c_p T_0 \eta \tag{4.1.6}$$

Bymaking use of Eq. (4.1.2) this equation leads to the important relationship

$$\boxed{v = a_0\sqrt{n\,\eta}} \tag{4.1.7}$$

Remark 1 Equation (4.1.7) *is known in literature as St. Venant–Wantzel equation*

$$v = \sqrt{\frac{2\kappa}{\kappa - 1}\frac{R}{M_p}T_0\left[1 - (p/p_0)^{\frac{\kappa-1}{\kappa}}\right]}$$

Remark 2 *Although* v_0 *is not exactly zero, the neglected tenn* $\frac{1}{2}m_p v_0^2$ *in* Eq. (4.1.6) *fonnally can be ascribed to the chamber temperature* via

$$T_0 \to T_0' = T_0 + \frac{1}{2}\frac{v_0^2}{c_p}$$

The expression $m_p c_p T_0'$ *is then the total combustion enthalpy.*

In the above we have made use of the expression for the sound velocity

$$a = \sqrt{\frac{\kappa p}{\rho}} = \sqrt{\frac{\kappa RT}{M_p}} = \sqrt{\frac{\kappa RT_0}{M_p}}\sqrt{\frac{T}{T_0}} =: a_0\sqrt{1-\eta} \quad \textbf{speed of sound} \tag{4.1.8}$$

as given by physics. The latter is a result of Eq. (4.1.3). Note that Eq. (4.1.7) is valid for the gas velocity at any point along the flow right down to the nozzle exit. Also note that a decreasing pressure or temperature leads to an increase of thermal

efficiency and also to an increasing flow velocity. We will have a closer look at this counter-intuitive behavior later on.

4.1.3 Flow at the Throat

We recall from Eq. (1.2.8) that the following continuity equation holds for the mass flow rate

$$\boxed{\dot{m}_p = \rho\, vA = const} \quad \textbf{continuity equation} \tag{4.1.9}$$

Since it is a result of mass conservation, the mass flow rate $\dot{m}_p$ must be constant over any cross section along the flow track.

Remark *Strictly speaking, we presume* $\dot{m}_p = const$ *from which an areal cross section is defined* via *the continuity equation, on which* ρ *und* v *are constant. If the gas jet diverges, i.e., is no longer axial, such as in the nozzle, the area is no longer flat, but in lowest approximation a sphere segment. The flow vector is normal to the surface of this segment. The center of the sphere is the imaginary point where the gas flow lines converge. Depending on whether the exiting jet is under- or over-expanding (see* Fig. 4.4 *and according text) the exit area is a convex or concave sphere segment, respectively.*

We now define the important parameter *mass flux* (a.k.a. *mass flow density)* $\mu := \dot{m}_p/A$. For μ we find from Eqs. (4.1.4), (4.1.7), and (4.1.8):

$$\mu := \frac{\dot{m}_p}{A} = a_0\rho_0\sqrt{n\eta(1-\eta)^n} = a\rho\sqrt{\frac{n\eta}{1-\eta}} \tag{4.1.10}$$

Because $\dot{m}_p = const$, μ is not constant. As mass flow is constant and the nozzle cross section has its minimum at the throat, the mass flux μ at a constant a_0 and ρ_0 has a maximum at the throat with

$$\eta_t = \frac{1}{n+1} \tag{4.1.11}$$

Equation (4.1.11) is easily derived by zeroing the first derivation of Eq. (4.1.10). By applying Eqs. (4.1.11) to (4.1.10) we find for the mass flux at the throat

$$\mu_t = \frac{\dot{m}_p}{A_t} = a_0\rho_0\sqrt{\left(\frac{n}{n+1}\right)^{n+1}} = a_t\rho_t \tag{4.1.12}$$

where the last term results from the last term of Eq. (4.1.10) due to $n\eta_t/(1-\eta_t) = 1$. In addition we get from Eqs. (4.1.9), (4.1.12), and (4.1.8) the flow velocity at the throat

$$v_t = \frac{\dot{m}_p}{\rho_t A_t} = \frac{\rho_t a_t A_t}{\rho_t A_t} = a_t = a_0\sqrt{\frac{n}{n+1}} \tag{4.1.13}$$

In words this is equivalent to the following:

> The flow velocity just reaches sound velocity at the throat. This is an essential property of thermal propulsion engines.

Note *Sound velocity at the throat here is not the conventional* $a_{air} \approx 343.4\ \mathrm{m\,s^{-1}}$ *at standard atmosphere, but due to* Eq. (4.1.8) $a_t = a_{air}\cdot\sqrt{T_t/T_{air}} \approx 1200\ \mathrm{m\,s^{-1}}$. *So,* a_t *is much bigger and in addition dependent on* T_t *and hence on the temperature and pressure conditions in the pressure chamber.*

Let us pause for a moment to ponder about what we have achieved so far, and what lies still ahead of us. Strictly speaking, the above maximum mass flux at the throat, and with it this whole chapter, describes a key property of a thermal thruster. In view of the maximization principle, the physical principle of mass conservation as expressed in Eqs. (4.1.9) and (4.1.10), and the conversation of energy (whose result led to Eq. (4.1.7)), all considerations following now are just more or less clever applications, new definitions and analytical conversions of Eqs. (4.1.7), (4.1.9), (4.1.10), and (4.1.12).

4.1.4 Flow in the Nozzle

Behind the throat, the gas expands into the widening nozzle (this constrictional geometry from the chamber through a narrow throat to a nozzle with an hourglass-shape that widens in the flow direction, is called a *Laval nozzle*, see Fig. 4.3) and exits the nozzle at the exit cross section A_e with velocity v_e. Obviously, the exit gas pressure p_e and v_e will depend on the expansion ratio A_e/A_t. Applying Eq. (4.1.10) to the nozzle exit and from Eq. (4.1.12) we find for this expansion ratio

$$\varepsilon := \frac{A_e}{A_t} = \frac{\dot{m}_p}{A_t}\frac{A_e}{\dot{m}_p} = \frac{a_0\rho_0\sqrt{\left(\frac{n}{n+1}\right)^{n+1}}}{a_0\rho_0\sqrt{n\,\eta_e(1-\eta_e)^n}}$$

So

$$\varepsilon := \frac{A_e}{A_t} = \frac{C_\infty}{n+2}\frac{1}{\sqrt{(1-\eta_e)^n \eta_e}} \quad \textbf{expansion ratio} \tag{4.1.14}$$

with

$$C_\infty := (n+2)\sqrt{\frac{n^n}{(n+1)^{n+1}}} \approx 0.624\frac{n+2}{\sqrt{n+1}} \quad \textbf{infinite–expansion coefficient}$$

where the latter follows for $n \approx 8$ from Problem 4.2. We call C_∞ the *infinite-expansion coefficient* for reasons, which will become clear in Sect. 4.3.2. For our standard $n = 8$ $(\kappa = 1.25)$ it has the value $C_\infty = 2.0810$.

Remark 1 In literature Eq. (4.1.14) reads

$$\varepsilon = \frac{A_e}{A_t} = \sqrt{\frac{\kappa-1}{2}\left(\frac{2}{\kappa+1}\right)^{\frac{\kappa+1}{\kappa-1}}} \cdot \left(\frac{p_0}{p_e}\right)^{1/\kappa}\left[1-\left(\frac{p_e}{p_0}\right)^{1-1/\kappa}\right]^{-1/2}$$

Remark 2 *In the literature the quantity* $\Gamma = C_\infty/\sqrt{n+2}$ *is sometimes called Vandenkerckhove Function.*

From Eq. (4.1.14) we see that there is a one-to-one correspondence between ε and η_e and due to Eq. (4.1.3) also between ε and all intensive thermodynamic variables p_e, T_e, ρ_e. We could therefore invert Eq. (4.1.14) to derive for a given ε the quantity $\eta_e(\varepsilon)$ and hence also $p_e(\varepsilon)$, $T_e(\varepsilon)$, $\rho_e(\varepsilon)$ via

$$\left(\frac{p_e(\varepsilon)}{p_0}\right)^{\frac{2}{n+2}} = \frac{T_e(\varepsilon)}{T_0} = \left(\frac{\rho_e(\varepsilon)}{\rho_0}\right)^{\frac{2}{n}} = 1-\eta_e(\varepsilon)$$

However, $\eta_e(\varepsilon)$ can be derived only numerically since the relation between η_e and ε is too convoluted. In Fig. 4.2, we therefore provide a graphical solution for η_e and p_e. It illustrates that η_e monotonously increases and hence p_e monotonously decreases with an increasing ε. Analogous diagrams can of course be drawn also for T_e and ρ_e. Because any cross section along the nozzle axis can be considered as a momentaneous exit, all these dependencies also holds along the nozzle axis. We can thus depicture the dependency of all intensive variables along a nozzle, which is done in Fig. 4.3.
From a practical point of view it is interesting to know how the expansion ratio changes if the chamber pressure is varied at $p_e = const$. From all the above we derive, after some minor algebra, that for small variations

$$\frac{\Delta\varepsilon}{\varepsilon} = \left[1-\frac{p_e}{2(p_0-p_e)}\right]\frac{\Delta p_0}{p_0} \approx \frac{\Delta p_0}{p_0}$$

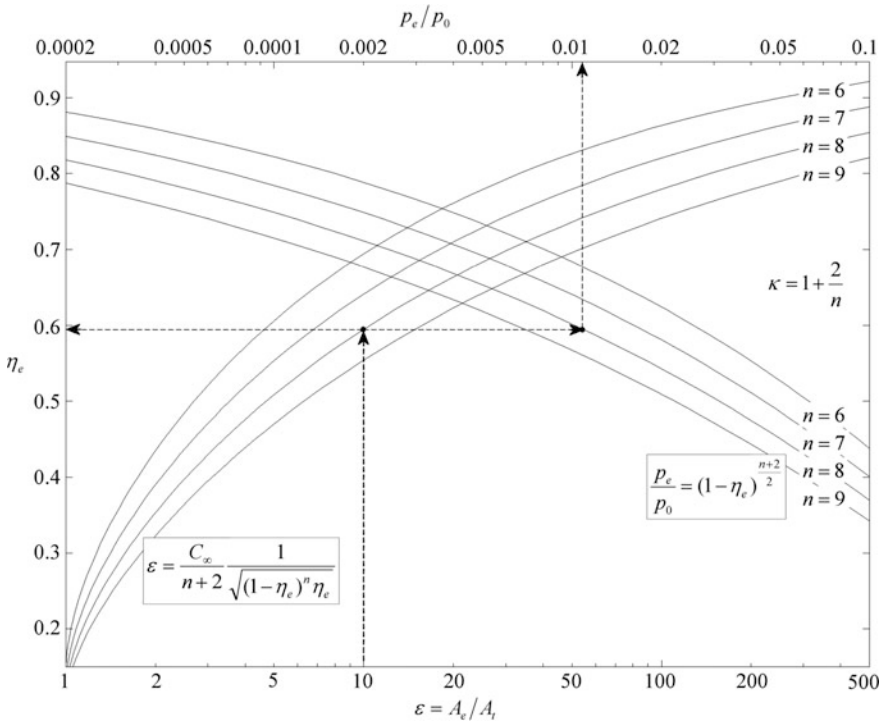

Fig. 4.2 Thermal efficiency η_e and pressure p_e at nozzle exit versus the expansion ratio ε for different excited degrees of freedom n of the gas molecules. In the figure shown is the example for $\varepsilon = 10$ and $n = 8$ leading to $\eta_e \approx 0.6$ and $p_e/p_0 \approx 0.01$

Flow velocity

According to Eqs. (4.1.3) and (4.1.7) the flow velocity increases with increasing expansion ratio (see Fig. 4.3). This is exactly what a nozzle is designed for. How big is this increase? The relation between the ejection velocity v_e and v_t can be derived from Eqs. (4.1.7) and (4.1.13) to be

$$v_e = a_0\sqrt{n\eta_e} = v_t\sqrt{n+1}\sqrt{\eta_e} \tag{4.1.15}$$

In other words:

> The velocity gain factor of a nozzle is $\sqrt{n+1}\sqrt{\eta_e} \approx 3\sqrt{\eta_e}$, which in vacuum tends to the value of 3. So a nozzle increases momentum thrust by 200%, but because the expansion at the same time reduces the pressure thrust, the gain in total thrust is less than 67% (see Sect. 4.3.3).

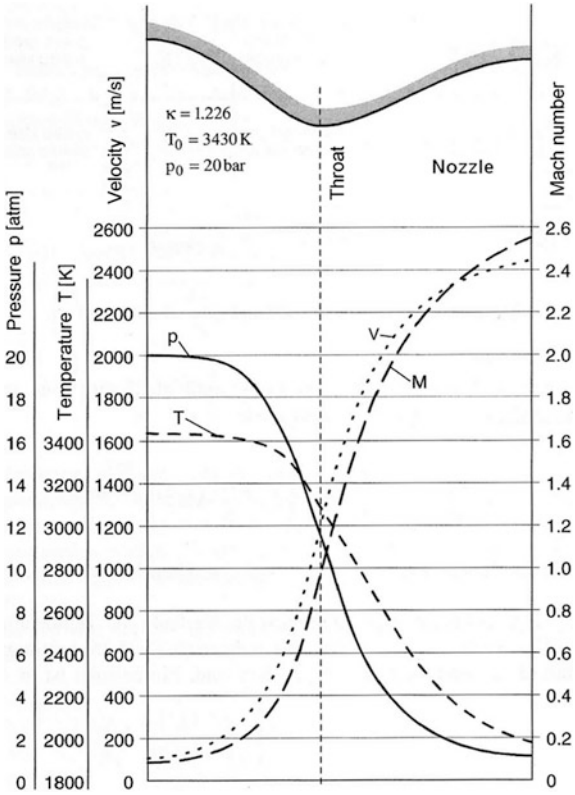

Fig. 4.3 Course of thermodynamic variables along a Laval nozzle. *Credit* Messerschmid, Fasoulas (2000)

It might be surprising to learn that the flow velocity increases with decreasing flow pressure. Intuitively, one would expect the contrary. Let us see why this seemingly paradoxical behavior occurs.

Hydrodynamics

This weird behavior is due to the hydrodynamic nature of the gas flow. The continuity Eq. (4.1.9)

$$\rho v A = const$$

hereby plays a key role. It states that, if the cross section A of the nozzle increases, the product ρv has to decrease. It now crucially depends on the dependence $\rho \propto 1/v^{\alpha}$, or equivalently its differential $d\rho/\rho = -\alpha \cdot dv/v$, and hence on the exponent α how v behaves: If $\alpha > 1$, then due to $\rho \cdot v \propto 1/v^{\alpha} \cdot v = v^{1-\alpha}$ v increases with increasing A, otherwise v decreases, or vice versa.

So we have to determine α to solve the paradox. We start out by examining the ideal gas Eq. (4.1.1), $p = \rho RT/M_p$, and the equation of energy conservation (4.1.6), $v^2 = 2c_p(T_0 - T)$. To arrive at one-to-one relations between the intensive thermodynamic variables p, ρ, T, v, which we are looking for, we need an additional relation between any two of them. This is furnished by the fact that according to thermodynamics for adiabatic processes $pV^\kappa = const$ holds. Because in general $\rho V = const$, we find $p \propto \rho^\kappa$ and hence

$$\frac{dp}{p} = \kappa \frac{d\rho}{\rho} \tag{4.1.16}$$

So p and ρ change in the same way: increasing p implies increasing ρ and vice versa (which we write in short as $p \uparrow \leftrightarrow \rho \uparrow$). In order to apply this differential equation, we have to differentiate $p = \rho RT/M_p$ and $v^2 = 2c_p(T_0 - T)$, which yields

$$\frac{dp}{p} = \frac{d\rho}{\rho} + \frac{dT}{T}$$

and

$$v\, dv = -c_p dT$$

With Eq. (4.1.16) we find the one-to-one relations

$$\frac{d\rho}{\rho}(\kappa - 1) = \frac{dT}{T} = -\frac{v^2}{c_p T}\frac{dv}{v} \tag{4.1.17}$$

Because $\kappa > 1$, they state the relationship $\rho \uparrow \leftrightarrow T \uparrow \leftrightarrow v \downarrow$. The latter inverse behavior, which seems quite strange, is due to the law of energy conservation, to which we will turn later. Because of Eqs. (4.1.2) and (4.1.8) it follows that $c_p(\kappa - 1)T = \kappa RT/M_p = a^2$ and hence

$$\frac{d\rho}{\rho} = -\frac{v^2}{a^2}\frac{dv}{v} = -(Ma)^2\,\frac{dv}{v} \tag{4.1.18}$$

where $Ma := v/a$ is the so-called **Mach number**. It is dimensionless by relating the flow velocity to the instantaneous speed of sound. With Eq. (4.1.18) we have identified $\alpha = (Ma)^2$. To find the explicit dependencies $v \leftrightarrow A$ and $\rho \leftrightarrow A$, we differentiate $\rho vA = const$ and get

$$\frac{d\rho}{\rho} + \frac{dv}{v} + \frac{dA}{A} = 0$$

Inserting Eq. (4.1.18) into this, we finally obtain

$$\frac{dv}{v} = \frac{1}{(Ma)^2 - 1}\frac{dA}{A} \quad \textbf{area–velocity equation} \tag{4.1.19}$$

or

$$\frac{d\rho}{\rho} = -\frac{(Ma)^2}{(Ma)^2 - 1}\frac{dA}{A}$$

From this we can read off the change of flow velocity as a function of change of cross section. We have to discern two cases:

1. subsonic case $(Ma < 1)$: $A \uparrow \rightarrow \rho \uparrow$ & $v \downarrow \leftrightarrow T \uparrow$
2. supersonic case $(Ma > 1)$: $A \uparrow \rightarrow \rho \downarrow$ & $v \uparrow \leftrightarrow T \downarrow$

In the subsonic case the flow velocity declines along the nozzle and its density increases, while for the supersonic case things are reverse.

Note *This implies that, if the flow would not reach sound velocity at the throat, the flow in the nozzle would stay subsonic and even decrease. The condition $v = a$ at the throat therefore is a critical condition for a thermal propulsion engine.*

Physical Interpretation

This leaves open the question, why the flow behaves so differently at subsonic and supersonic speeds. This is due to the kinetic energy of the flow. Let us take a look at the law of energy conservation of the gas as given by Eq. (4.1.5)

$$m_p c_p T + \frac{1}{2} m_p v^2 = const$$

It shows that the kinetic energy increases quadratically with flow velocity. So any change in gas temperature implies decreasing flow speed changes for increasing flow speeds. This is expressed explicitly in Eq. (4.1.17): relative density and temperature changes are rigidly coupled, while the coupling between temperature and speed changes is quadratically in v. Therefore, for a given $\Delta\rho/\rho$ and with increasing v the absolute value of $\Delta v/v$ decreases.

So, overall the following happens. The space available for a given amount of gas enlarges with increasing cross section along the nozzle, $A \uparrow$. Thereby the density and the speed of the gas, flowing into the enlarging space ahead of it, change such that the amount of gas remains constant (conservation of mass, $\rho v A = const$). If the density would increase, $\rho \uparrow$, then due to $\rho v A = const$, the flow speed v would have to strongly decrease, $v \downarrow\downarrow$. But at supersonic speeds this is not possible, because due to the gas equation $\rho \uparrow \leftrightarrow T \uparrow$ and because of the equation of energy conservation v decreases only little. Only at subsonic flow speeds the flow speed reduction would be big enough to compensate. Therefore at supersonic speeds the density has to drop, $\rho \downarrow$, causing the gas temperature via the gas equation to drop as well, which in turn raises the flow speed only little, $v \uparrow$. But this is all what is necessary according to $\rho v A = const$ because the density reduction already counteracts the increase of cross section to a large amount.

From the above equation of energy conservation with implication $T \uparrow \leftrightarrow v \downarrow$ one can read off another important feature: the first term is enthalpy, which is the internal microscopic kinetic energy plus displacement work pV, and the second term is the kinetic flow energy of the gas. But because temperature is a direct measure of the translational microscopic motion of the gas molecules, as seen early on in this chapter, the inverse dependency can be interpreted in the following way:

> Supersonic expansion along the nozzle converts part of the microscopically disordered motion of the molecules (microscopic translations) into an increasingly macroscopically directed motion (flow velocity) of the gas.

In view of the second law of thermodynamics, which always demands that entropy increases and hence implies a decreasing motional order, one may ask how an increasingly directed motion can form from random motion. The answer is that the second law of thermodynamics holds for a gas in equilibrium. In a diverging nozzle just behind the throat, where gas molecules move at and above the speed of sound, the gas is in a highly non-equilibrium phase. Physics (see e.g. Reimann (2002)) has shown that a non-equilibrium gas in an asymmetric structure, such as a bell nozzle that causes an asymmetric potential in which the molecules move, can approach equilibrium by rectifying random motion into orderly directed molecular flow along the asymmetry line. This effect is known as *fluctuation-driven transport*.

Upon temperature reduction, fewer rotational and vibrational modes of the gas molecules are excited. By means of impact processes they decay into microscopic translations thus adding slightly to the flow velocity of the gas. However, this additional conversion effect, which lowers the excited degrees of freedom n and adds to the nozzle efficiency (see Sect. 4.3.3), is not considered in our derivations. We assume that n or κ is constant with temperature.

4.2 Ideally Adapted Nozzle

4.2.1 Ideal-Adaptation Criterion

A nozzle is designed to increase ejection velocity. However, our goal is not to maximize ejection velocity, but thrust. In order to do so, let us have a look at the expression for total thrust. If the exit surface normal $\boldsymbol{u}_e$ and $\boldsymbol{v}_e$ go into the same directionamount of total thrust of a real engine according to Eq. (1.2.14) (for the sake of simplicity we drop the average sign throughout this section)

$$F_* = \eta_{div}\dot{m}_p v_e + (p_e - p_\infty)A_e$$

Expanding the gas through the nozzle not only increases v_e but also reduces p_e. The first term on the right-hand side tells us that this implies an increase of the momentum thrust, but the second term leads to a reduction of the pressure thrust. So, what we really want to know is how to choose p_e or v_e to maximize the thrust as the combined force of momentum thrust and pressure thrust.

Our optimization problem is even a bit more complicated. According to the above equation, thrust depends on three parameters, p_e, v_e, and A_e, if the mass flow rate is considered to be constant. The latter assumption is generally admissible, as supersonic speed in the nozzle has the positive effect that erratic flow variations cannot expand backward into the combustion chamber. The Laval nozzle acts like a barrier, and the mass flow rate of the propulsion is only determined by the pressure in the combustion chamber and the diameter of the exit (see Eq. (4.3.2)). It is our long term goal to find that optimal combination of $p_{e,opt}$, $v_{e,opt}$, and $A_{e,opt}$ for which thrust is maximum.

Mathematically speaking optimization means that we are looking for that combination where any variations δA_e, δv_e, and δp_e do not lead to any further increase of F_*, that is, $\delta F_* = 0$. If we consider infinitesimally small variations, this can be expressed mathematically by the total differential as follows:

$$dF_* = dF_A + dF_e + dF_p = \frac{\partial F_*}{\partial A_e} dA_e + \frac{\partial F_*}{\partial v_e} dv_e + \frac{\partial F_*}{\partial p_e} dp_e = 0 \qquad (4.2.1)$$

Deriving the partial derivatives from Eq. (1.2.14) we find

$$dF_* = \left(p_{e,opt} - p_\infty\right) dA_e + \eta_{div} \dot{m}_p dv_e + A_{e,opt} dp_e = 0$$

We now consider the fact that the thermodynamic variables v_e and p_e are directly dependent on each other via Eqs. (4.1.15) and (4.1.3). With these relationships and with application of Eq. (4.1.10) we can calculate (exercise, Problem 4.1) the derivation dv/dp straightforwardly. Alternatively, Eq. (4.1.16) can be inserted into Eqs. (4.1.17) and (4.1.9) applied. In both cases one obtains

$$dv = -\frac{A}{\dot{m}_p} dp$$

This relation describes the change of flow velocity with pressure at any cross section A along the nozzle while the mass flow rate $\dot{m}_p$ is constant. Interestingly, it states that the flow velocity increases at decreasing gas pressure (see discussion of this effect in Sect. 4.1.4). Applying this equation to the nozzle exit and inserting it into the above equation yields

$$dF_* = \left(p_{e,opt} - p_\infty\right) dA_e + (1 - \eta_{div}) A_{e,opt} dp_e = 0$$

This brings us to the required condition for maximum thrust:

$$\frac{dA_e}{dp_e} = -\frac{(1-\eta_{div})A_{e,opt}}{p_{e,opt}-p_\infty}$$

From Eq. (4.1.14) we derive that

$$\frac{dA_e}{dp_e} = -\frac{A_{e,opt}}{p_0}\frac{1}{n+2}\frac{n-(1-\eta_e)}{\eta_e(1-\eta_e)^{n/2+1}}$$

and therefore we obtain for the optimal exit pressure

$$\begin{aligned}\frac{p_{e,opt}}{p_\infty} &= 1-\frac{p_0}{p_\infty}(1-\eta_{div})(n+2)\frac{\eta_e(1-\eta_e)^{n/2+1}}{n-(1-\eta_e)}\\ &= 1-(1-\eta_{div})\frac{(n+2)\eta_e}{n-(1-\eta_e)}\\ &\approx 1-(1-\eta_{div})\underbrace{\frac{10\eta_e}{7+\eta_e}}_{0.79-1.25}\end{aligned}$$

The second equation follows from Eq. (4.1.3) and is exact. The last holds because $n \approx 8$, and because $\eta_{div} \approx 1$ we have $p_{e,opt} \approx p_\infty = 0-1\ b$. From Eq. (4.1.3) and typically $p_0 \approx 100\ b$ hence it follows that $\eta_e = 1.0-0.6$. We therefore find approximately

$$p_{e,opt} \approx \eta_{div} p_\infty \tag{4.2.2}$$

and the maximal thrust is

$$F_{*,\max} = \eta_{div}\dot{m}_p v_{e,opt} - p_\infty(1-\eta_{div})A_{e,opt}$$

and

$$\eta_{e,opt} = 1-\left(\eta_{div}\frac{p_\infty}{p_0}\right)^{\frac{2}{n+2}}$$

For an ideal engine with $\eta_{div} = 1$ we thus can state that

> The thrust (propellant force) for an ideal thermal engine achieves its maximum for $p_e = p_\infty$, i.e., when the pressure thrust vanishes.

Remark *We actually only showed that F_* is optimal at $p_e = p_\infty$. For the proof that it really is maximal see* Fig. 4.7 *in* Sect. 4.3.2.

4.2.2 Ideal Nozzle Design

For $p_e = p_\infty$ the corresponding *optimal* ejection *velocity* can be derived from Eq. (4.1.15) as

$$v_{e,opt} = a_0\sqrt{n\eta_{e,opt}} \approx a_0\sqrt{n\eta_\infty} \tag{4.2.3}$$

By the same token, we derive from $p_e = p_\infty$ and hence $\eta_e \to \eta_\infty$ the optimal expansion ratio ε_{opt} from Eq. (4.1.14) to be

$$\varepsilon_{opt} = \frac{A_{e,opt}}{A_t} = \frac{C_\infty}{n+2}\frac{1}{\sqrt{\left(1-\eta_{e,opt}\right)^n \eta_{e,opt}}} \approx \frac{C_\infty}{n+2}\frac{1}{\sqrt{(1-\eta_\infty)^n\eta_\infty}} \quad \textbf{optimal expansion ratio} \tag{4.2.4}$$

Because we rather are pursuing $A_{e,opt}$ the question remains: Given Eq. (4.2.4) what is the design value of the throat cross section A_t to obtain $A_{e,opt}$? We will answer this question in Sect. 4.4.1. Thus, we have finally determined the optimal parameters $p_{e,opt}$, $v_{e,opt}$, and $A_{e,opt}$.

Flow Expansion

A nozzle that achieves $p_e = p_\infty$ is called an **ideally adapted nozzle**. In a nozzle where the optimum is not achieved, be it $p_e < p_\infty$, which is called *over-expansion* because the jet is over expanded within the nozzle (see Fig. 4.4), or $p_e > p_\infty$, called *under-expansion* because the jet was not able to properly expand within the nozzle, divergences arise behind the nozzle exit. The jet direction then is not longer parallel to the engine axis. This leads to a loss of thrust, as there are thrust components perpendicular to the engine axis, which are then irreversibly lost. Depending on the altitude, the I_{sp} losses due to non-adapted nozzles are typically in the range 0–15%. As pressure adiabatically lowers with increasing volume, thrust reductions due to an over- or under-expanding jet can be counteracted by an increase or decrease of the exit surface, which is equivalent to extending or reducing the length of the Laval nozzle.

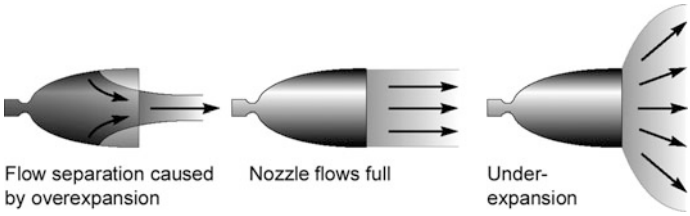

Fig. 4.4 Flow conditions of an over-expanding (left), ideally expanding (middle), and under-expanding (right) nozzle

4.2.3 Shock Attenuation and Pogos

For an ideally adapted nozzle $dF_* = dF_e + dF_p = 0$. Therefore $dF_p = -dF_e$ must hold. In other words, every tiny pressure thrust variation is counterbalanced by a momentum thrust variation. This is quite a remarkable effect, as pressure variations occur within every combustion chamber in the form of shock waves, which travel from the combustion chamber right beyond the nozzle exit. The reverse interdependency $dF_p = -dF_e$ ensures that none of these shock waves has any effect on the total thrust.

The situation is different with pogos, which are the nightmare of thruster manufacturers—and astronauts. Pogos are thrust oscillations along the engine axis, which may put the rocket under enormous stress even beyond its structural limits. As astronaut Michael Collins stated, "The first stage … vibrated longitudinally so that someone riding on it would be bounced up and down as if on a pogo stick." Pogos result from a negative feedback between thrust and mass flow rate. Assume, for instance, that at a given time a an unsteady combustion causes a temporary larger heat release and therefore an increase of chamber pressure. This partially impedes the propellant flow into the chamber, which in turn results in local and even overall pressure decrease in the chamber. The transient pressure build up in the propellant supply lines in combination with the pressure drop inside the chamber yields an increase in propellant mass flow rate (note that due to differences in propellant densities and velocities there will be a phase shift between the two mass flow rates). The frequency of this pogo resonance usually is of the order of 10 Hertz. The partial blocking of the flow rate yields a local extinction of the flame. The influx of unburnt propellant into the hot environment quite often results in a sudden reaction (explosion) with an appropriate heat release and local pressure build-up which starts the cycle again.

Pogos are not taken care of in our above considerations, as we assumed a constant mass flow rate. A small accumulator connected to the fuel line, as for instance the pogo suppressor with about the size of a basketball charged with hot gaseous oxygen in the Shuttle orbiter, as shown in the Fig. 4.5 usually damps them out, because it gives and takes additional propellant depending on the acceleration on the propellant and hence on the fuel pressure in the fuel line.

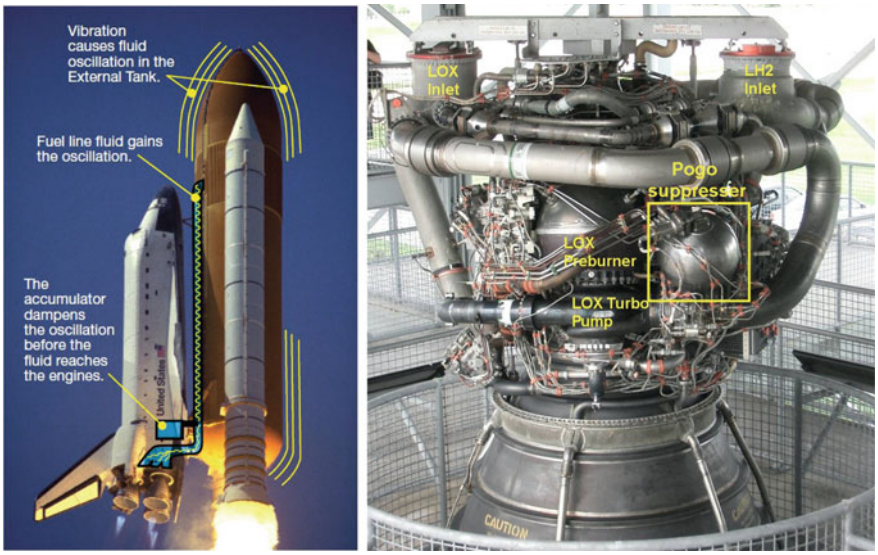

Fig. 4.5 Pogo resonance (left) and pogo suppressor system (right) in the SSME of the Space Shuttle

4.2.4 Ideal Engine Performance

According to Sect. 1.3.3 engine performance and hence rocket performance is measured very generally by the engine's figure of merit: the specific impulse $I_{sp} = v_*/g_0$. Now that we have derived an expression for the ejection velocity of thermal engines, we are ready to determine their I_{sp} from thermodynamic values. Usually I_{sp} is cited in literature for an ideally adapted nozzle in vacuum. At these conditions we get a *maximum obtainable specific impulse*, which can be calculated from Eq. (4.1.15) for $p_e = p_\infty = 0$. This yields with Eq. (4.1.8)

$$g_0 I_{sp,\max} = v_{e,\max} = a_0\sqrt{n} = \sqrt{(n+2)\frac{RT_0}{M_p}} = \sqrt{\frac{2h_0}{M_p}} \quad @\ \text{vacuum} \tag{4.2.5}$$

where $h_0 = M_p H_0/m_p$ is the molar form of the available enthalpy H_0, which comprises the combustion enthalpy H_p (heat of reaction) of the propellant with **combustion efficiency** η_c, that is, $\eta_c H_p$, and the externally supplied energy E_{ext}

$$H_0 = \eta_c H_p + E_{ext} \tag{4.2.6}$$

η_c is determined by the heat losses of the engine, which are quite considerable (see Fig. 4.6). From Eqs. (4.2.5) and (4.2.6) we get the remarkably simple result

For an ideally adapted engine in vacuum, its maximum specific impulse does not depend on the design of the engine or the chamber pressure, but it depends exclusively on the propellant properties and the combustion efficiency of the engine. The best propellant is a propellant with the highest combustion molar enthalpy h_p and lowest molar mass M_p.

Because H_2/O_2 displays one of the highest molar enthalpies and hydrogen has the lowest molar mass, it fuels chemical thrusters with the highest efficiency available. Apart from employing a better propellant, the specific impulse can only be further increased at a given mass flow rate by utilizing the combustion enthalpy as much as possible in the combustion chamber (e.g., by a more efficient precombustion), or by injecting additional external energy (e.g., external nuclear–thermal energy), or by reducing heat losses.

Total Engine Efficiency

The total engine efficiency of a propulsion engine is a measure for the effectiveness of converting the energy released into the combustion chamber E_{in} into exhaust energy (kinetic energy of the exhaust jet). We recall from Eq. (1.3.7) that for $v_e(\theta) \approx const = v_e$ it is given as $\eta_{tot} = \frac{1}{2} m_p v_e^2 / E_{in}$. Without any supply of external energy, one then obtains

$$\eta_{tot} = \frac{m_p v_e^2}{2\eta_c H_p} = \left(\frac{v_e}{v_{e,\max}} \right)^2 \quad @\ E_{ext} = 0 \tag{4.2.7}$$

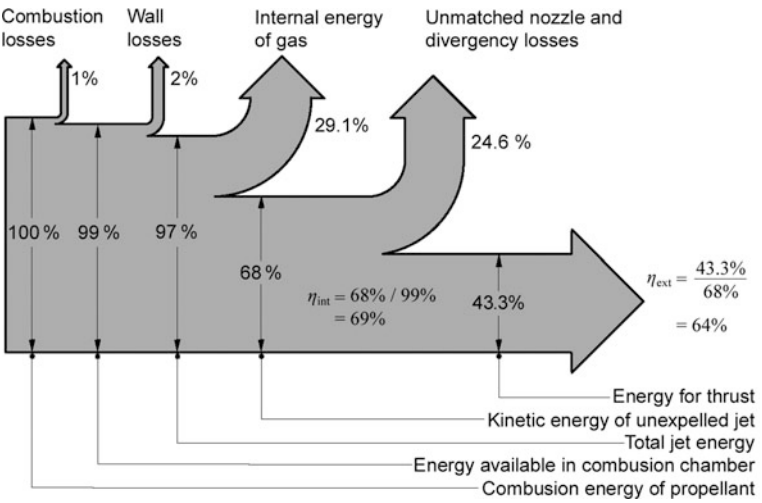

Fig. 4.6 Energy flow of the third stage engine of Ariane 1

Example

The SSME cryogenic engine of the Space Shuttle burned H_2/O_2 with $\eta_c H_p/m_p = 13.4\,\mathrm{MJ/kg}$, i.e., $v_{e,\max} = 5.18\,\mathrm{km/s}$, and exhausted the propellant with $v_e = 4.44\,km/s$. The internal efficiency therefore was $\eta_{tot} = 0.735$, which, equaling the Russian RD-0120 engine. was, and still is the best value for chemical engines.

4.3 Engine Thrust

We saw above that the figure of merit of an engine, $I_{sp,\max}$, does not depend on the engine design, the chamber pressure in particular. The all-important thrust on the other hand does. How does the thrust depend on the engine design? We recall from Eq. (1.2.14) that the thrust of an ideal engine having $v_{ex} = v_e$ is given by

$$F_* = \dot{m}_p v_e + (p_e - p_\infty)A_e$$

Inserting $v_e = a_0\sqrt{n\eta_e}$ from Eq. (4.1.15) we get for the thrust

$$F_* = \dot{m}_p a_0\sqrt{n\eta_e} + (p_e - p_\infty)A_e \tag{4.3.1}$$

How is the mass flow rate $\dot{m}_p$ related to chamber pressure p_0? To figure this out, we apply Eq. (4.1.12)

$$\dot{m}_p a_0\sqrt{n} = a_0^2\rho_0 A_t n\sqrt{\frac{n^n}{(n+1)^{n+1}}}$$

Since $a_0^2\rho_0 = \kappa p_0$ (see Eq. (4.1.8)) and because $\kappa n = n+2$ we get the important relation

$$\dot{m}_p = \frac{A_t C_\infty}{a_0\sqrt{n}}p_0 \tag{4.3.2}$$

where C_∞ is the infinite-expansion coefficient defined in Eq. (4.1.14) . Because of Eq. (4.3.2) we now can rewrite thrust more conveniently for engineering purposes as

$$\boxed{F_* = p_0 A_t C_\infty\sqrt{\eta_e} + (p_e - p_\infty)A_e} \tag{4.3.3}$$

For an ideally adapted nozzle with $p_e = p_\infty$ we have $\eta_e = \eta_\infty$ and thus we find for the thrust

$$F_* = p_0 A_t C_\infty\sqrt{\eta_\infty} \quad @\ p_e = p_\infty \tag{4.3.4}$$

In vacuum the thrust of an ideally adapted engine achieves its maximum value

$$F_* = p_0 A_t C_\infty \quad @\ p_e = p_\infty = 0 \tag{4.3.5}$$

This is merely a theoretical value, as the nozzle exit cross section A_e would then grow infinitely big, as we see from Eq. (4.1.14).

4.3.1 Engine Performance Parameters

Characteristic Velocity c^*

Chamber pressure, propellant mass flow rate, and cross section of the throat need to be in balance to each other. With a larger cross section of the throat, the mass flow rate has to rise, in order to maintain the chamber pressure. Equation (4.3.2) describes the interplay between these three parameters. Their ratio determines the so-called *characteristic velocity* (commonly pronounced "cee-star")

$$c^* := \frac{p_0 A_t}{\dot{m}_p} = \frac{a_0\sqrt{n}}{C_\infty} = \frac{1}{C_\infty}\sqrt{\frac{2h_0}{M_p}} = \frac{g_0 I_{sp,\max}}{C_\infty} = const \tag{4.3.6}$$

characteristic velocity

Because both C_∞ and $I_{sp,\max}$ depend only on propellant properties, c^* is constant and an alternative figure of merit for the engine. From Eq. (4.3.6) and because from Eq. (4.2.6) $h_0 = \eta_c h_p$ it follows that c^* can be considered as a parameter to rate the propellant combustion performance, i.e. the energy level of the propellant, the burn efficiency of the injector, and the heat loss efficiency of the chamber. In practice, the value of c^* for a given propellant and thrust chamber design is guessed from existing experience and refined during development testing.

Given Eq. (4.3.6) the ejection velocity from Eq. (4.1.15) can be written as

$$v_e = c^* C_\infty \sqrt{\eta_e} = g_0 I_{sp,\max}\sqrt{\eta_e} \tag{4.3.7}$$

Thrust Coefficient C_f

Equation (4.3.3) gives rise to the definition of the so-called *thrust coefficient* C_f, which is of high practical importance for engine design:

$$C_f := \frac{F_*}{p_0 A_t} \tag{4.3.8}$$

The rationale is that according to Eq. (4.3.6) the product $p_0 A_t = \dot{m}_p c^* = const$ for $\dot{m}_p = const$. Therefore, when optimizing an engine design at a given fuel

consumption only C_f matters. Comparing Eqs. (4.3.3) with (4.3.8) and applying Eq. (4.3.6), we derive the following expression for C_f

$$C_f = \frac{v_*}{c^*} = C_\infty \sqrt{\eta_e} + \frac{p_e - p_\infty}{p_0}\frac{A_e}{A_t} \quad \textbf{thrust coefficient} \tag{4.3.9}$$

The thrust coefficient is a dimensionless parameter used to measure the gas expansion performance through the nozzle, i.e. the design quality of the nozzle. According to Sect. 4.1.4, both η_e and p_e/p_∞ are a function of $\varepsilon = A_e/A_t$. alone. Therefore, $C_f(\varepsilon, p_0/p_\infty)$.

One might assume that $p_0 A_t$ might be the thrust of just the chamber and C_f is an efficiency factor that accounts for the nozzle contribution. As we will see in Sect. 4.3.3, C_f is not the nozzle efficiency factor but is directly related to it. So C_f just has engineering and no physical relevance.

Characteristic velocity and thrust coefficient are two key engine parameters for design engineers. So it is worth investigating what the actually achievable values for these two parameters are. For $p_0 A_t = set$ we therefore find from Eqs. (4.3.6) and (4.3.8) and the results of Sect. 1.3.3, the correction factors

$$\eta_{c^*} := \frac{\text{actual } c^*}{\text{ideal } c^*} = 1/\frac{\text{actual } \dot{m}_p}{\text{ideal } \dot{m}_p} = \frac{1}{\zeta_d} = 0.87 - 1.02$$

$$\eta_f := \frac{\text{actual } C_f}{\text{ideal } C_f} = \frac{\text{actual } F_*}{\text{ideal } F_*} = \eta_T = \eta_{div} = 0.92 - 1.00$$

4.3.2 Thrust Performance

Let us examine the thrust at a given fuel consumption, i.e., for $\dot{m}_p = const$. We rewrite Eq. (4.3.3) with Eqs. (4.3.8) and (4.3.6) as

$$\boxed{F_* = c^* \dot{m}_p C_f(\varepsilon, p_0/p_\infty)} \tag{4.3.10}$$

In order to determine the thrust performance we thus only need to determine $C_f(\varepsilon, p_0/p_\infty)$. We do so by solving Eq. (4.1.14) for $\eta_e(\varepsilon)$ (cf. Fig. 4.2), and plug the result into Eq. (4.3.9). However, this can be done only numerically, the result of which is depicted in Fig. 4.7. Recall from Sect. 4.1.4 that $\Delta\varepsilon/\varepsilon = [1 - O(p_e/p_0)]\,\Delta p_0/p_0 \approx \Delta p_0/p_0$. The nearly horizontal curves display the change of the thrust coefficient with the expansion ratio ε at a given chamber pressure ratio p_0/p_∞. The curves confirm our theoretical conclusion from Sect. 4.2.1 that maximal thrust occurs at $p_e = p_\infty$ indicated by the line crossing all others. The region around the thrust maximum, in particular for high combustion chamber pressures, is so flat that a slightly suboptimally adapted nozzle does not gravely reduce thrust.

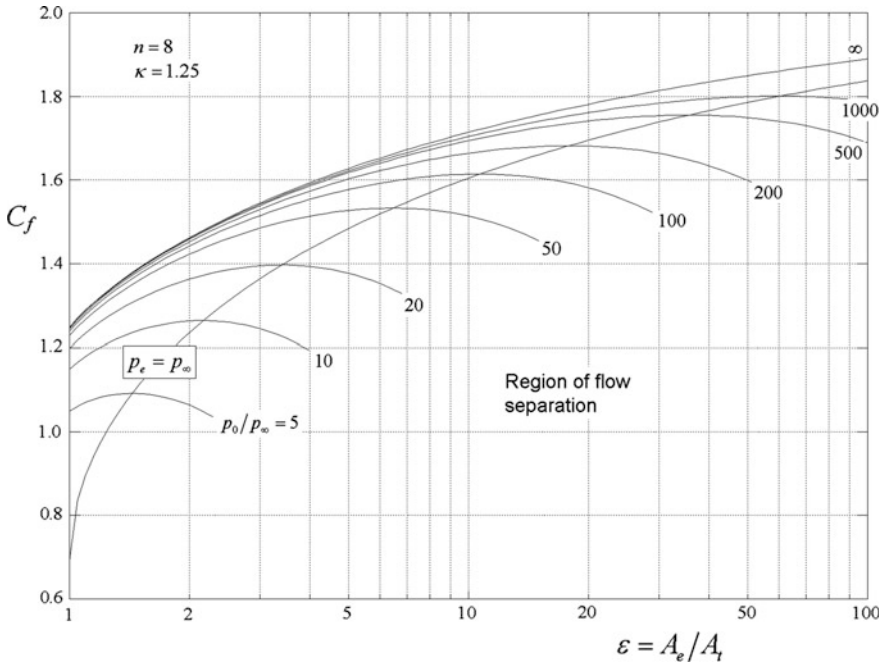

Fig. 4.7 The dependence of the thrust coefficient C_f on the expansion ratio ε for $n = 8$ ($\kappa = 1.25$)

Nevertheless, in course of the ascent through the atmosphere into space, over-expansion and under-expansion losses on average are about 10%.

Figure 4.7 shows that the thrust coefficient C_f steadily increases until for $A_e/A_t \to \infty$, i.e., in vacuum ($\eta_e \to \eta_\infty = 1$), $C_f = C_\infty = 2.0810$. In this case the infinitely sized nozzle allows the exhaust jet to expand to zero ambient pressure, which is why we call C_∞ infinite-expansion coefficient. Likewise the thrust tends to its limiting value of Eq. (4.3.5).

Thrust Sensitivity Analysis I—Dependence on Chamber Pressure

We now want to study the dependence of the thrust from key chamber design parameters.

We first analyze the thrust variations of an ideally adapted engine for varying chamber pressure at a given $\dot{m}_p = const$. To have the engine remain ideally adapted, the pressure thrust must remain zero and therefore $p_e = p_\infty = const$. Because ε is to be adjusted such that $p_e = p_\infty$ the only variable according to Eq. (4.3.10), is p_0, which from Eq. (4.3.6) corresponds to a variable A_t, namely $dp_0/p_0 = -dA_t/A_t$. Due to $F_* = c^* \dot{m}_p C_f = c^* \dot{m}_p C_\infty \sqrt{\eta_\infty}$ we then have

$$\frac{dF_*}{F_*} = \frac{dC_f}{C_f} = \frac{1}{2}\frac{d\eta_\infty}{\eta_\infty} = \left(\frac{p_0}{2\eta_\infty}\frac{d\eta_\infty}{dp_0}\right)\frac{dp_0}{p_0}$$

From $\eta_\infty = 1 - (p_\infty/p_0)^{\frac{2}{n+2}}$ follows that

$$\frac{p_0}{2\eta_\infty}\frac{d\eta_\infty}{dp_0} = \frac{1}{n+2}\frac{1-\eta_\infty}{\eta_\infty} = \frac{1}{n+2}\frac{1}{(p_0/p_\infty)^{\frac{2}{n+2}}-1}$$

and therefore the relative change of the thrust is

$$\begin{aligned}\frac{\Delta F_*}{F_*} &= \frac{1}{n+2}\frac{1-\eta_\infty}{\eta_\infty}\frac{\Delta p_0}{p_0} \\ &= -\frac{1}{n+2}\frac{1}{(p_0/p_\infty)^{2/(n+2)}-1}\frac{\Delta A_t}{A_t}\end{aligned} \quad @\ \begin{matrix} p_e = p_\infty \\ \dot{m}_p = const \end{matrix} \tag{4.3.11}$$

So, the increase in efficiency is notably effective for low chamber pressures. We find for $n = 8$ and for a typical pressure ratio $p_0/p_\infty \approx 75/0.5 = 150$, $\eta_\infty \approx 0.63$ and hence

$$\frac{\Delta F_*}{F_*} \approx 0.06\,\frac{\Delta p_0}{p_0} = -0.06\,\frac{\Delta A_t}{A_t} \quad @\ \begin{matrix} p_e = p_\infty \\ \dot{m}_p = const \end{matrix}$$

Thrust Sensitivity Analysis II—Dependence on Mass Flow Rate
An interesting case in point is when the thrust of an engine changes just due to a variation in mass flow rate (propellant injection rate). We then have $\varepsilon = const \rightarrow \eta_e = const \rightarrow v_e = const$. From $\eta_e = 1 - (p_e/p_0)^{2/(n+2)}$ then follows

$$p_e = p_0(1-\eta_e)^{\frac{n+2}{2}} = \dot{m}_p c^*(1-\eta_e)^{\frac{n+2}{2}}\varepsilon.$$

Therefore

$$F_* = \dot{m}_p v_e + (p_e - p_\infty)A_e = \dot{m}_p\left[v_e + c^*(1-\eta_e)^{\frac{n+2}{2}}\varepsilon\right] - p_\infty A_e$$

and with Eqs. (4.3.2) and (4.3.7)

$$\begin{aligned}\frac{dF_*}{d\dot{m}_p} &= v_e + c^*(1-\eta_e)^{\frac{n+2}{2}} \\ &= c^*\left(C_\infty\sqrt{\eta_e} + \frac{p_e}{p_0}\varepsilon\right) = c^*\left(C_f + \frac{p_\infty}{p_0}\varepsilon\right)\end{aligned} \quad @\ \varepsilon = const$$

With $F_* = \dot{m}_p v_* = \dot{m}_p c^* C_f$ and with Eq. (4.3.9) the relative thrust change as a function of a relative propellant injection rate change therefore is

$$\frac{\Delta F_*}{F_*} = \left(1 + \frac{p_\infty \varepsilon}{C_f p_0}\right) \frac{\Delta \dot{m}_p}{\dot{m}_p} \quad @\ \varepsilon = const$$

For $p_e = p_\infty$, $\eta_\infty \approx 0.63$ (see above), and with Eq. (4.2.4)

$$\frac{p_\infty \varepsilon}{C_f p_0} = \frac{(1-\eta_\infty)^{(n+2)/2}}{C_\infty \sqrt{\eta_\infty}} \varepsilon_{opt} = \frac{1}{n+2} \frac{1-\eta_\infty}{\eta_\infty} \approx 0.06 \quad @\ p_e = p_\infty$$

we alternatively have

$$\frac{\Delta F_*}{F_*} = \left(1 + \frac{1}{n+2} \frac{1-\eta_\infty}{\eta_\infty}\right) \frac{\Delta \dot{m}_p}{\dot{m}_p} \approx 1.06 \frac{\Delta \dot{m}_p}{\dot{m}_p} \quad @\ \begin{matrix} p_e = p_\infty \\ \varepsilon = const \end{matrix} \tag{4.3.12}$$

So, mainly the momentum thrust contributes while the pressure thrust (0.06) contributes only little owing to deviations from the ideally adapted nozzle induced by the change in the mass flow rate.

4.3.3 Nozzle Efficiency

The thrust coefficient might be of engineering interest, but it does not provide an answer to the ultimate question: What is the thrust a nozzle adds to the engine performance? We therefore define the nozzle coefficient (nozzle efficiency) as follows:

$$C_n := \frac{thrust\ of\ an\ engine\ with\ nozzle}{thrust\ of\ an\ engine\ without\ nozzle} = \frac{F_*}{F_{*,plain}} \tag{4.3.13}$$

by assuming no divergence losses in both cases, i.e. $\eta_{div} = 1$. According to Eq. (1.2.14), an engine without nozzle would provide the thrust

$$F_{*,plain} = \dot{m}_p v_t + (p_t - p_\infty) A_t$$

From Eqs. (4.1.11), (4.1.3), and (4.3.2) we find for the pressure at the throat

$$p_t = p_0 \left(\frac{n}{n+1}\right)^{\frac{n+2}{2}} = p_0 \frac{n}{\sqrt{n+1}} \frac{C_\infty}{n+2} \approx 0.55 \cdot p_0$$

With the relation $v_t = a_0 \sqrt{n} / \sqrt{n+1}$ from Eq. (4.1.13) and with $\dot{m}_p a_0 \sqrt{n} = p_0 A_t C_\infty$ from Eq. (4.3.2) we can rewrite it to

$$F_{*,plain} = p_0 A_t C_\infty \left(\frac{1}{\sqrt{n+1}} + \frac{n}{\sqrt{n+1}} \frac{1}{n+2} - \frac{p_\infty}{C_\infty p_0} \right) = p_0 A_t \left(\frac{2C_\infty \sqrt{n+1}}{n+2} - \frac{p_\infty}{p_0} \right) \tag{4.3.14}$$

As shown in Problem 4.2 at any practical rate

$$2C_\infty \frac{\sqrt{n+1}}{n+2} = 1.25$$

Therefore we arrive at the interesting result that an engine without nozzle provides the thrust

$$F_{*,plain} = p_0 A_t \left(1.25 - \frac{p_\infty}{p_0} \right) \approx 1.2 \cdot p_0 A_t \tag{4.3.15}$$

The latter is due to $p_\infty / p_0 \approx 0.01$. For the thrust of an engine with nozzle, Eq. (4.3.8) states that $F_* = p_0 A_t C_f$. If we insert this equation and Eq. (4.3.14) into Eq. (4.3.13) we obtain

$$C_n = \frac{C_f}{\frac{2C_\infty \sqrt{n+1}}{n+2} - \frac{p_\infty}{p_0}} \approx \frac{C_f}{1.25 - \frac{p_\infty}{p_0}} \tag{4.3.16}$$

with

$$C_f = \frac{v_*}{c^*} = C_\infty \sqrt{\eta_e} + \frac{p_e - p_\infty}{p_0} \frac{A_e}{A_t}$$

We therefore arrive at the approximation adequate at any practical rate

$$\boxed{C_n \approx 0.81 \cdot C_f} \quad \textbf{nozzle coefficient} \tag{4.3.17}$$

The nozzle efficiency thus can be estimated to be 81% of the thrust coefficient. Because $F_* = C_n \cdot F_{*,plain}$ and in comparison to $F_* = C_f \cdot p_0 A_t$ the nozzle coefficient C_n is a more vivid substitute for C_f. The two are virtually in a direct relation to each other.

If the nozzle is ideally adapted, then $C_f = C_\infty \sqrt{\eta_\infty}$, and we get

$$C_n = \frac{C_\infty \sqrt{\eta_\infty}}{1.25 - p_\infty / p_0} \quad @\ p_e = p_\infty \tag{4.3.18}$$

For a nozzle ideally adapted to outer space one gets from Eq. (4.3.16) with $C_f = C_\infty$

$$C_n = \frac{n+2}{2\sqrt{n+1}} \approx \frac{5}{3} = 1.667 \quad @\ p_e = p_\infty = 0 \tag{4.3.19}$$

Thus, in space a nozzle ideally adapted to vacuum always increases the thrust by approximately 67% independent of the pressure in its combustion chamber. However, this is an ideal case because a nozzle adapted to vacuum in space would have an infinite size. Because $p_e = p_\infty = 0$ is a limiting condition, therefore, the nozzle efficiency in general is always lower than 67%.

Example

The Space Shuttle SSME LH2/LOX engine had $I_{sp}(vacuum) = 455\ s$, $I_{sp}(1\ bar) = 363\ s$, and $c^* = 2330\,m/s$. Therefore, during ascent through Earth's atmosphere, one gets $1.53 \leq C_f \leq 1.91$ and thus $1.23 \leq C_n \leq 1.53$. So, a SSME nozzle provides at sea level 23% and in space 53% more engine thrust.

4.4 Engine Design

For engine design, aspects of maximum performance, engine reliability, cost, and, last but not least, system constraints need to be considered. An engine design for a reusable launch system for instance has to be a compromise between efficiency and durability. An optimum engine design may even contradict an optimum system design. As an example consider the mixture ratio of LOX/LH2 engines. While the engine designer would favor a mixture ratio around 5, which corresponds to maximum specific impulse and slightly lower hot gas temperatures, stage or launcher architects favor higher mixture ratios, which result in in significantly lower LH2 tank volumes, however at the expense of a lower specific impulse and a higher hot gas temperature. Therefore, every engine usually is unique in that it is tailored to the specific requirements of a rocket for a mission.

Despite these many design aspects this section deals only with the layout of an engine to achieve maximum total thrust. We already know two engine parameters that govern engine geometry: the cross-sectional area of the combustion chamber throat, A_t, and the cross-sectional area of the nozzle exit, A_e. In order to optimize the engine layout we need to design both, combustion chamber and nozzle. Let us go into details.

4.4.1 Combustion Chamber

Equation (4.3.6) determines the design of the combustion chamber: On the left-hand side of the equation we have the technically variable parameters, on the right-hand side we only have propellant-specific parameters. For instance, with a given (turbo pumps, combustion rate) mass flow rate $\dot{m}_p$, and a maximum

admissible pressure of the combustion chamber p_0, we can determine the necessary cross section A_t of the throat

$$A_t = \frac{\dot{m}_p}{p_0 C_\infty}\sqrt{\frac{2h_0}{M_p}} = \frac{F_*}{p_0 C_\infty \sqrt{\eta_\infty}} \tag{4.4.1}$$

The chamber volume V_c remains undefined by these considerations. It only comes into play when internal combustion processes are analyzed. Then the so-called *characteristic length* (commonly pronounced "L-star")

$$L^* = \frac{V_c}{A_t} \quad \textbf{characteristic length} \tag{4.4.2}$$

plays an important role. From the continuation Eq. (4.1.9) we derive for the chamber volume $V_c = \dot{m}_p t_s/\rho$, where t_s is the propellant residence time in the chamber. Hence, essentially $L^* \propto t_s$. Experimentally, the characteristic velocity c^* increases monotonically with L^* to an asymptotic maximum, due to better mixing and burning on its path through the chamber. On the other hand, longer thrust chambers result in higher weight and more chamber surface area to be cooled (typically by fuel) and more friction losses. Yet, in expander cycle engines a minimum surface is needed in order to extract sufficient heat from the chamber to drive the turbines. If the chamber is too long resonances may occur, which cause standing pressure waves, so-called *thrust oscillations*, a problem which became widely known in early 2008 in the course of the solid-fuel boosters design phase of NASA's Ares I rocket. Therefore, the choice of the right L^* is subject to quite contradictory requirements.

Without going into details of a chamber stability analysis, we may mention that typically $L^* = 0.76 - 1.02$ m for LOX/LH2 engines, $L^* = 1.02 - 1.27$ m for LOX/RP-1 engines, and $L^* = 0.76 - 0.89$ m for hydrazine-based N_2O_4 engines (see Humble et al. (1995)). Optimum L^* relies on past experience and evaluation of actual firings of experimental thrust chambers. If we assume a common cylindrical combustion chamber with cross section A_c and length L_c, i.e., $V_0 = A_c L_c$, and follow the rough relationship for chamber contraction ratio

$$\frac{A_c}{A_t} = 7.44\left(A_t/1\,\mathrm{cm}^2\right)^{-0.3} + 1.25 \tag{4.4.3}$$

suggested by Huzel and Huang (see Humble et al. (1995, p. 222)), which is based on engine test data and simple gas-dynamic considerations, the chamber length should be scaled as

$$L_c = \frac{V_c}{A_c} = L^*\frac{A_t}{A_c} = \frac{L^*}{7.44(A_t/1\,\mathrm{cm}^2)^{-0.3} + 1.25} \tag{4.4.4}$$

In general, it can be said that in solid-fuel boosters with their very high characteristic length longitudinal waves leading to thrust oscillations are a standing problem. In liquid thrusters these modes are dampened out by the throat (no pressure reflection) at the back-side and by the injection system and propellant distribution devices and even by the injected droplets (droplet drag) itself acting as active acoustic elements on the front side of the chamber. Therefore transversal, rather than longitudinal, waves play a major role here.

In closing we note that although computer codes today sufficiently simulate selected combustion processes such as propellant vaporization, mixing, and combustion, there currently exists no end-to-end approach to determine the optimal fuel injection mechanism and chamber configuration from scratch. Good engine design still relies on a substantial amount of experimental data that makes it a laborious undertaking. This is why one often falls back on existing reliable engines such as for the Ares I and Ares V rockets, which were slated for the canceled US Constellation program.

4.4.2 Nozzles

One essential result of our engine design considerations for an ideal rocket (ideal rocket criteria see Sect. 4.1.1) is that according to Eq. (4.3.10), thrust depends (see also Fig. 4.7) just on the expansion ratio ε via the parameter p_0. So, the nozzle design is determined solely by the areal ratio of its end faces, and not by its exact shape in between. In fact, from a thermodynamic point of view, the shape of the nozzle casing and how the gas expands in it is irrelevant as long as the gas flow is one-dimensional and expands steadily and adiabatically. So any smooth contour that precludes shock formation will do. This purports that the nozzle should not expand too rapidly behind the throat, implying that the angle of the nozzle casing against the nozzle axis should not be too large. From an engineering point of view, a well-designed shape can reduce the mechanical strain of the nozzle along its axis.

For a real rocket any nozzle design has to respect that the gas exhibits a two-dimensional flow pattern (radial and axial dependence), that the shape of the divergent supersonic part dictates shock formation and hence performance gain/loss, and that there are boundary layer losses due to friction with the nozzle wall. For instance, accounting for the latter a shorter nozzle may reduce the thermodynamic thrust gain, but increases total thrust gain due to less boundary losses in addition to less weight and less side loads at engine start-up (see bell nozzle below).

We do not want to go into details about these implications for the nozzle shape, but mention the four principal nozzle designs.

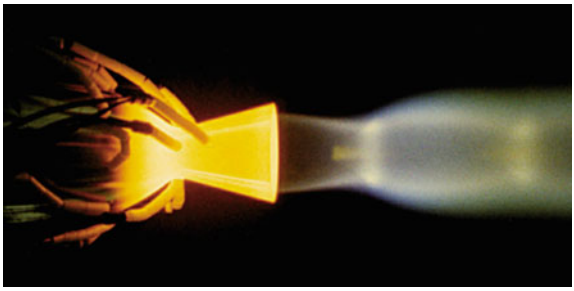

Fig. 4.8 A small chemical thruster with conical nozzle. *Credit* DLR

Conical Nozzle

If mechanical strain is not an issue, for instance for engines with little thrust, simple conical nozzles are a practical solution (see Fig. 4.8). They are simple to design and manufacture. However, they lead to some thrust losses due to oblique shocks at the discontinuous transition from the throat to the cone 12°–18°. The conical nozzle with a 15° divergent half-angle has become almost a standard because it is a good compromise on the basis of weight, length, and performance.

Bell Nozzle

The most common contoured nozzle is the bell-shaped nozzle (see Fig. 4.9). The shape, which usually is a parabolic-geometry approximation, is ideal because the gases quickly expand conically (angle of expansion typically 30°–60°) behind the throat. The expansion waves emanating from this quick expansion diminish the compression effects caused by the flow reorientation, thereby leading to relatively little nozzle losses. The longer the gases run along the nozzle, the less divergence occurs because of the bell shape, and at the exit the gases are expelled almost parallel to the nozzle axis. A near optimal thrust bell nozzle contour uses the parabolic approximation procedures suggested by Rao (1958), in particular

Fig. 4.9 Bell nozzle of the Aestus upper stage engine from Ariane 5 with CC-NE I/F. *Credit* ESA/Arianespace

the so-called thrust-optimized parabolic (TOP) nozzles, used for instance for the Vulcain, J-2S, and SSME engines.

Combustion and Start-Up Instabilities

During engine start-up significant lateral off-axis loads, so-called side loads, as shown in Fig. 4.10 occur in a thrust-optimized contour nozzle, which are of quite a complex nature. They are caused by

1. combustion waves of hydrogen-rich jet afterburning in the nozzle, the transversal component of which hits the wall, thereafter by
2. the oscillation of the supersonic jets of the Mach disk flow and subsequent axial oscillation of the Mach disk itself, then by
3. asymmetric flow separation patterns of types FSS (free-shock separation), RSS (restricted-shock separation), and FSS-to-RSS transitions caused on one hand by over-expansion (recall that at launch elevation the nozzle is overexpanding) and on the other by the Coanda effect, which draws the supersonic core jet to the wall, and finally by
4. asymmetric lip lambda shock oscillation.

In outer space, where the thrust reaches its maximum, the thrust force may lead to axial buckling of the nozzle (Fig. 4.10). Axial buckling of the, at that time, new Vulcain 2 engine was the reason for the total failure of Ariane 5 ECA on December 11, 2002.

During engine start-up 10% of the thrust level is due to side loads. They can be reduced by ideal contoured nozzles, which are usually less sensitive towards flow separation during start-up. In addition, the danger of nozzle damage due to side-load deformations and buckling deformations increases with decreasing nozzle size and hence with decreasing distance to the throat. So, shorter nozzles do less damage.

Owing to this load situation, the cross over from the heavy reinforced combustion chamber (CC), to the lighter nozzle extension (NE), the so-called CC-NE I/F, is not

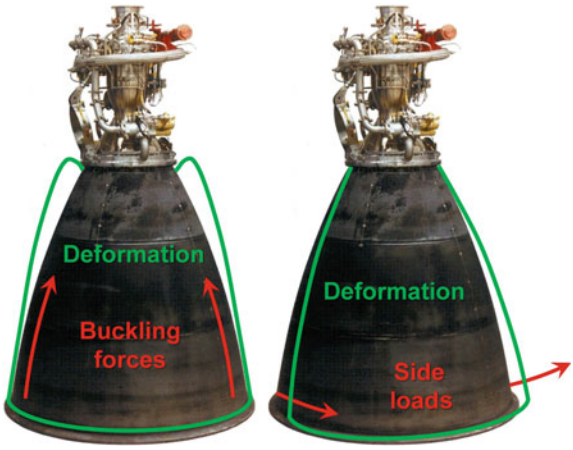

Fig. 4.10 Deformations of a Bell nozzle caused by buckling forces at high altitudes (left) and side loads at engine start-up (right)

at the throat, but is located farther downstream (see Fig. 4.8). Its actual location is always a compromise between the weight of the thruster and its tolerance for deformation loads.

An equivalent 15° half-angle conical nozzle is commonly used as a standard to specify bell nozzles. For instance, the length of an 80% bell nozzle (distance between throat and exit plane) is 80% of that of a 15° half-angle conical nozzle having the same throat area, radius below the throat, and area expansion ratio.

Both conical and Bell nozzles belong to the class of so-called convergent-divergent nozzles (CD nozzle, a.k.a. Laval nozzle), where the gas flow is convergent before the throat and divergent after the throat.

Circular Nozzles

In circular nozzles (a.k.a. annular nozzles) combustion occurs along a ring, or annulus, around the base of the nozzle. There are two basic types of circular nozzles:

1. *Radial outflow nozzles* where the exhaust is expanded radially outward such as in the expansion-deflection (E-D) (Fig. 4.11), reverse-flow (R-F), and horizontal-flow (H-F) nozzles.
2. *Radial inflow nozzles* where the exhaust is expanded radially inward, such as the spike nozzle (a.k.a. *(full-length radial) plug nozzle*) (Fig. 4.12) and aerospike nozzle (a.k.a. *truncated (radial) plug nozzle*).

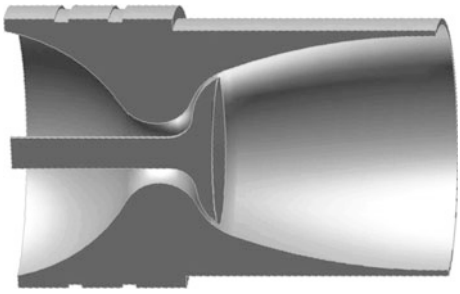

Fig. 4.11 Cutaway view of an expansion–deflection nozzle with a pintle deflecting the flow outward toward the wall. *Credit* RedHotIceCube, Creative Commons

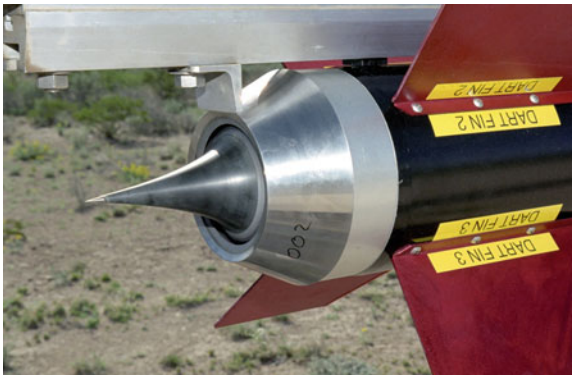

Fig. 4.12 A spike nozzle having a plug at the center as used in NASA's Dryden Aerospike Rocket Test in March 2004. *Credit* NASA

The radial outflow nozzle has an inner free-jet boundary with the outer nozzle wall contour (see Fig. 4.8). Conversely, radial inflow nozzles have an inner but no outer wall, the latter is just the outer surface of the annular flow as a free-jet boundary, which is self-adjusted by ambient pressure. Compared to a bell-shaped nozzle, annular nozzles are more complex to design but operate more efficiently across a wide range of altitudes.

For a **plug nozzle** (spike nozzle) the word "plug" refers to the center body that blocks the flow from what would be the center portion of a traditional nozzle (see Fig. 4.12).

An **aerospike nozzle** is a plug nozzle with a truncated plug. The term "aerospike" follows from the fact that the virtual bell is formed on the inner side by the spike and on the other by the air. Since this property holds also for the plug nozzle, both terms are often used interchangeably. However, aerospike was originally used only for a truncated plug nozzle. As a result of the truncation, the turbulent wake, which at high altitudes would form aft of the base, results in a high base drag and reduced efficiency. This drawback can greatly be alleviated by a "base bleed" into the region aft of the base forming an "air spike".

Circular nozzles suffer from large surfaces which have to be cooled and problems with non-symmetric combustion owing to uneven annular distribution of the exhaust gases. This results in thrust vector diversion and local shock waves leading to local heat load peaks and hence temperature peaks. To prevent thruster damage the entire plug area needs to be overly cooled.

Linear Nozzles

Plug nozzles and aerospike nozzles also come in the form of linear nozzles, where the combustion occurs in a line.

In a **linear aerospike engine**, such as the hailed Rocketdyne RS-2200 (Fig. 4.13), many small combustion chambers are placed in a line along two sides of the truncated straight spike nozzle. Throttling of either side therefore allows

Fig. 4.13 Test run of the linear aerospike engine RS-2200 at Rocketdyne. *Credit* NASA-MSFC

steering of the engine. The disadvantages of the linear aerospike are severe heat losses and thrust divergences and hence thrust losses at the two open sides of the engine, which could be prevented by winglets, but those would again need to be cooled.

4.4.3 Design Guidelines

The essential of this section is summarized by the following coarse engine design guidelines:

1. Choose fuel and oxidizer (h_0, n, M_p) from efficiency and practical considerations. From this follows

$$C_\infty := (n+2)\sqrt{\frac{n^n}{(n+1)^{n+1}}}$$

2. Choose the altitude and hence the external pressure p_∞ to which the engine should be ideally adapted: $p_e = p_\infty$
3. Determine the required total engine thrust F_* (at the altitude to which the engine is to be adapted).
4. Choose the chamber pressure p_0 from thruster efficiency (see Fig. 4.7) and chamber material considerations (such as strength and thermal conductivity), and that the chamber volume scales with (see Eqs. (4.4.2) with (4.3.6))

$$V_c = L^* A_t = \frac{L^* c^* F_*}{v_* p_0} \propto \frac{F_*}{p_0}$$

5. From this and from Eqs. (4.3.4) and (4.2.4) follows

$$\eta_\infty = 1 - \left(\frac{p_\infty}{p_0}\right)^{2/(n+2)}$$

$$A_t = \frac{F_*}{p_0 C_\infty \sqrt{\eta_\infty}}$$

$$A_e = \frac{C_\infty}{n+2} \frac{A_t}{\sqrt{(1-\eta_\infty)^n \eta_\infty}}$$

6. Finally and as described in Sect. 4.4.1 choose with the chosen fuel and oxidizer the characteristic length of the chamber L^*. With this the chamber length L_c and its cylindrical diameter D_c should be

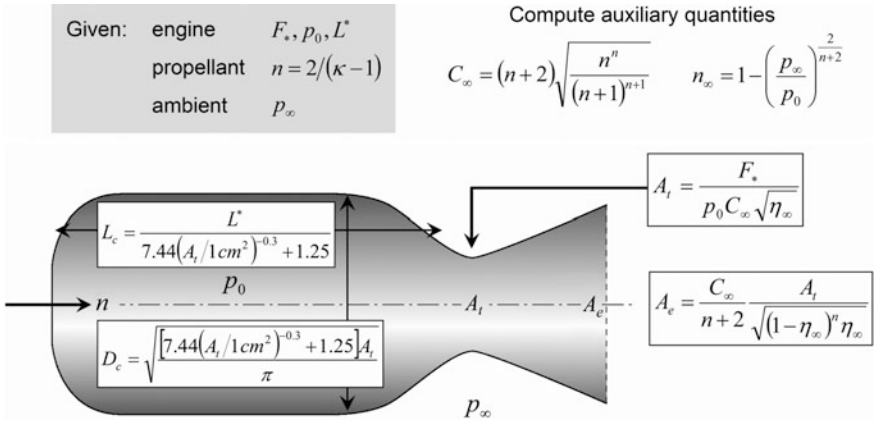

Fig. 4.14 Design flow to determine the optimal engine design

$$L_c = \frac{L^*}{7.44(A_t/1\ \mathrm{cm}^2)^{-0.3} + 1.25}$$

$$D_c = 2\sqrt{\frac{\left[7.44(A_t/1\ \mathrm{cm}^2)^{-0.3} + 1.25\right]A_t}{\pi}}$$

Obviously, the choice of the fuel and oxidizer, a properly chosen external pressure p_∞, chamber pressure p_0, and characteristic length L^*, i.e., finding the detailed dimensions of the pressure chamber, is of high importance and requires a lot of expertise.

In Fig. 4.14, the design guidelines are outlined as a workflow to determine the optimal engine design.

4.5 Problems

Problem 4.1 *Gas Velocity-Pressure Relation in a Nozzle*
Prove explicitly with Eqs. (4.1.7) and (4.1.3) and by applying Eq. (4.1.10) that for the gas velocity–pressure dependence in a nozzle holds

$$dv = -\frac{A}{\dot{m}_p} dp$$

Problem 4.2 *Approximation of the Infinite-Expansion Coefficient*
Prove that for $n \approx 8$ at any practical rate

$$C_\infty = \frac{36}{35\sqrt{e}} \frac{n+2}{\sqrt{n+1}} \left(1 - \frac{n-8}{315} + O\left(n^2\right)\right) \approx 0.624 \frac{n+2}{\sqrt{n+1}}$$

Hint: Consider the expression

$$\frac{n+2}{C_\infty \sqrt{n+1}} = \sqrt{\left(\frac{n+1}{n}\right)^n}$$